

## 29. ELECTRON MICROPROBE AND THERMOMAGNETIC ANALYSIS OF BASALT SAMPLES FROM HOLE 597C<sup>1</sup>

Tadashi Nishitani, Institute of Mining Geology, Mining College, Akita University, Akita, Japan<sup>2</sup>

### ABSTRACT

Electron microprobe and thermomagnetic analyses of selected basalt samples from Hole 597C were performed. The main purpose of this work was to investigate and estimate the degree of oxidation of the samples using the ratios of Fe to Ti and the Curie temperatures obtained from thermomagnetic curves. The results show that the magnetic properties of samples from Hole 597C change at a sub-bottom depth of 100 m, and that low-temperature and high-temperature oxidation processes prevailed above and below 100 m, respectively.

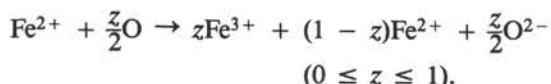
### INTRODUCTION

The degree of oxidation of a rock holds a key to the thermal history of the rock. Weathering processes and thermal effects can change the magnetic properties of a rock. Thermomagnetic analysis, which indicates the change in saturation magnetization as a function of temperature, can also directly indicate the degree of alteration. A rock sample which was never altered shows almost the same thermomagnetic curves during heating and cooling. The Curie temperature (or Curie point) is determined from the thermomagnetic curve as the intersection of tangents drawn above and below the smooth extensions at each side of the curve's inflection.

Two oxidation processes are involved in the oxidation of titanomagnetites: high- and low-temperature oxidation.

High-temperature oxidation is a decomposition process and produces observable lamellae, titanium-rich rhombohedral phases, and iron-rich spinel (Buddington and Lindsley, 1964; Hauptman, 1974). The spinel is dominant in the rock's magnetic properties and shows a Curie temperature of more than 500°C in the heating process of thermomagnetic analysis. The thermomagnetic cooling curve is almost the same as the heating curve.

Low-temperature oxidation of titanomagnetites is a process of converting from the stoichiometric state to the cation-deficient state. For low-temperature oxidation, the degree of oxidation is represented by the oxidation parameter  $z$  defined as the fraction of original  $\text{Fe}^{2+}$  converted to  $\text{Fe}^{3+}$ :



$z = 0.0$  indicates stoichiometric titanomagnetite and  $z = 1.0$  indicates the fully oxidized state (Ozima and Sakamoto, 1971). The Curie temperature generally increases

as the degree of low-temperature oxidation increases; that is, as  $z$  increases (Nishitani and Kono, 1983). The cation-deficient phase is unstable when heated above 400 to 450°C, and consequently it decomposes to an iron-rich stoichiometric titanomagnetite (spinel phase) and a hemo-ilmenite (rhombohedral phase) during the thermomagnetic heating process. Saturation magnetization ( $J_s$ ) increases with the addition of iron-rich titanomagnetite, but  $J_s$  decreases as the temperature approaches the Curie point. Therefore, a peak can be observed in the heating curve. The saturation magnetization during cooling shows a sharp rise owing to the new phase. In summary, typical low-temperature oxidation products show the characteristic feature of thermomagnetic curves, a peak during heating and a sharp rise during cooling (Ozima and Ozima, 1971). Some samples show lower Curie temperatures in a cooling cycle than in a heating cycle, depending on the sample size (Hamano et al., 1980).

We investigated the state of oxidation of 24 basalt samples from Hole 597C using electron microprobe and thermomagnetic methods. As already mentioned, we are able to interpret from thermomagnetic analysis whether a rock sample has been affected by a high- or low-temperature oxidation process or by no oxidation process at all. Using the ratios of Fe to Ti and titanomagnetite compositions determined by electron microprobe analyses, we can also obtain information on the degree of oxidation at low temperatures from the Curie temperature observed in a heating cycle (Nishitani and Kono, 1983).

### RESULTS OF ELECTRON MICROPROBE ANALYSES

Two hundred and four points were analyzed from 24 samples using an electron microprobe analyzer (JXA-5). Analyzed components were  $\text{FeO}$ ,  $\text{TiO}_2$ ,  $\text{Al}_2\text{O}_3$ ,  $\text{MgO}$ ,  $\text{MnO}$ ,  $\text{CaO}$ ,  $\text{SiO}_2$ , and  $\text{K}_2\text{O}$ . Qualitative analysis showed no trace of Na (sodium) and V (vanadium). Some samples were analyzed quantitatively for As (arsenic) and S (sulfur); their quantities were not detected, however, except as pyrrhotite. Correction factors were calculated according to the method of Bence and Albee (1968).

Results are summarized in Table 1. The mean values of each component are shown in Table 2; parentheses in-

<sup>1</sup> Leinen, M., Rea, D. K., et al., *Init. Repts. DSDP*, 92: Washington (U.S. Govt. Printing Office).

<sup>2</sup> Address: Institute of Mining Geology, Mining College, Akita University, Akita 010, Japan.

Table 1. Results of electron microprobe analysis, Hole 597C samples.

Core-Section interval (cm)	Analysis no. <sup>a</sup>	FeO	TiO <sub>2</sub>	Al <sub>2</sub> O <sub>3</sub>	MgO	MnO	CaO	SiO <sub>2</sub>	K <sub>2</sub> O	Sum	Fe/(Fe + Ti)	Note <sup>b</sup>
3-1, 131-134	A 1	71.45	17.09	2.41	1.17	0.77	0.04	0.42	0.02	93.37	0.823	
	2	71.97	16.71	2.17	0.96	0.66	0.06	0.31	0.02	92.86	0.827	
	3	72.71	17.30	2.32	1.23	0.67	0.03	0.32	0.02	94.62	0.824	
	4	72.72	16.96	2.32	1.19	0.63	0.06	0.47	0.03	94.39	0.827	
	B 1	76.65	18.46	2.48	1.06	0.43	0.02	0.14	0.02	99.26	0.822	
	2	75.27	18.99	2.38	0.98	0.43	0.03	0.14	0.02	98.23	0.815	
	3	71.38	19.77	2.37	0.91	0.44	0.05	0.39	0.03	95.33	0.801	
	4	71.27	19.02	2.79	0.91	0.41	0.08	0.33	0.02	94.82	0.807	
	5	72.09	19.48	2.48	0.71	0.41	0.06	0.23	0.02	95.48	0.805	
	A 1	73.75	20.74	2.04	0.35	0.52	0.02	0.13	0.02	97.57	0.798	
3-2, 40-43	2	74.42	20.77	1.87	0.32	0.55	0.03	0.15	0.01	98.13	0.799	
	3	73.80	21.18	1.86	0.35	0.50	0.07	0.16	0.03	97.93	0.795	
	B 1	73.86	20.45	2.03	0.27	0.48	0.03	0.18	0.02	97.34	0.801	
	2	73.79	20.54	2.17	0.33	0.52	0.03	0.78	0.03	98.20	0.800	
	3	73.90	20.52	2.25	0.33	0.53	0.02	0.16	0.02	97.73	0.800	
	D	74.13	18.08	2.19	0.24	0.56	0.03	0.01	—	95.25	0.820	
3-3, 5-8	A 1	59.80	24.79	1.87	0.41	0.59	0.50	3.46	0.07	91.49	0.729	
	2	60.55	24.20	1.92	0.53	0.57	0.39	3.08	0.06	91.30	0.736	
	3	54.07	26.51	1.70	0.61	0.55	0.71	4.19	0.06	88.40	0.694	
	4	59.94	24.50	1.80	0.48	0.61	0.32	2.74	0.07	90.47	0.731	
	B 1	50.16	31.02	1.80	0.87	0.36	1.63	5.89	0.08	91.81	0.643	
	2	59.30	25.89	2.02	0.67	0.47	0.60	2.98	0.06	91.99	0.718	
3-3, 52-55	3	62.36	22.84	2.31	0.68	0.43	0.48	3.47	0.07	92.64	0.752	
	4	67.19	21.88	2.30	0.53	0.44	0.27	1.69	0.06	94.36	0.774	
	D	70.67	15.98	2.12	1.35	0.79	0.04	0.60	—	91.56	0.831	
	A 1	65.65	22.54	2.28	0.27	0.54	0.06	0.52	0.05	91.91	0.764	
	2	65.64	23.08	1.94	0.26	0.59	0.06	0.25	0.03	91.85	0.760	
	3	65.74	22.46	2.05	0.26	0.57	0.05	0.20	0.04	91.36	0.765	
4-1, 60-63	B 1	67.05	21.90	2.76	0.28	0.45	0.11	0.28	0.03	92.86	0.773	
	2	67.77	22.08	2.65	0.25	0.55	0.15	0.23	0.02	93.70	0.773	
	3	66.45	21.81	3.00	0.28	0.49	0.13	0.82	0.06	93.04	0.772	
	A 1	65.04	22.33	2.64	0.79	0.57	0.09	0.14	0.02	91.61	0.764	
	2	68.35	20.50	2.94	0.85	0.49	0.04	0.14	0.02	93.32	0.788	
	3	69.33	21.34	2.99	0.96	0.44	0.04	0.05	0.02	95.16	0.783	
4-2, 111-114	4	68.39	22.12	2.74	0.77	0.43	0.02	0.10	0.02	94.58	0.775	
	B 1	67.95	21.51	2.72	0.95	0.57	0.06	0.16	0.02	93.92	0.778	
	2	68.20	22.31	2.50	0.85	0.51	0.04	0.11	0.02	94.55	0.773	
	3	68.57	21.81	2.68	0.92	0.47	0.02	0.07	0.02	94.56	0.778	
	4	62.28	19.80	2.14	1.03	0.60	0.12	7.12	0.70	93.78	0.778	
	A 1	72.85	20.36	2.22	0.31	0.51	0.40	0.00	0.02	96.32	0.799	
4-3, 27-30	2	73.20	20.78	2.05	0.31	0.64	0.03	0.56	0.03	97.61	0.797	
	3	68.99	24.42	2.14	0.62	0.55	0.12	0.62	0.01	97.47	0.759	
	B 1	72.68	20.09	2.12	0.25	0.53	0.04	0.00	0.02	95.72	0.801	
	2	70.35	21.08	2.08	0.39	0.55	0.07	0.00	0.02	94.54	0.788	
	3	72.07	21.04	1.63	0.23	0.56	0.07	0.00	0.01	95.62	0.792	
	4	71.80	20.42	2.25	0.39	0.58	0.10	0.00	0.02	95.55	0.796	
4-4, 76-79	A 1	73.91	20.26	1.97	0.25	0.57	0.03	0.07	0.01	97.07	0.802	
	2	71.88	19.90	2.21	0.34	0.46	0.03	0.07	0.02	94.90	0.801	
	3	73.47	19.45	1.97	0.33	0.50	0.06	0.07	0.02	95.86	0.808	
	B 1	74.50	19.48	2.33	0.69	0.52	0.03	0.05	0.02	97.60	0.810	
	2	74.50	18.75	2.57	0.75	0.44	0.02	0.01	0.01	97.06	0.815	
	3	74.02	19.84	2.28	0.28	0.57	0.01	0.01	0.02	97.04	0.806	
5-1, 129-132	A 1	69.71	21.05	2.69	0.42	0.59	0.04	0.17	0.02	94.69	0.787	
	2	69.23	21.65	2.10	0.37	0.67	0.05	0.12	0.03	94.21	0.781	
	3	73.23	16.38	3.97	0.61	0.43	0.09	0.17	0.03	94.92	0.833	
	B 1	69.58	22.37	2.28	0.60	0.54	0.04	0.08	0.02	95.52	0.776	
	2	69.97	22.18	2.49	0.56	0.60	0.02	0.14	0.03	95.98	0.778	
	3	69.78	22.55	2.06	0.32	0.68	0.04	0.20	0.03	95.64	0.775	
5-2, 63-66	A 1	59.78	25.81	1.72	0.52	0.52	0.38	2.36	0.07	91.15	0.720	
	2	58.67	26.16	1.72	0.58	0.57	0.43	2.33	0.05	90.52	0.714	
	3	57.83	26.24	1.73	0.56	0.52	0.52	3.15	0.07	90.62	0.710	
	4	58.93	25.63	1.70	0.54	0.57	0.46	3.19	0.07	91.09	0.719	
	5	58.11	26.38	1.81	0.59	0.44	0.64	3.70	0.07	91.74	0.710	
	B 1	51.00	27.74	1.44	0.62	0.40	0.96	3.93	0.12	86.20	0.672	
5-3, 27-30	2	53.96	27.13	1.58	0.54	0.56	0.62	3.00	0.08	87.46	0.689	
	3	54.86	26.37	1.64	0.53	0.42	0.66	3.33	0.10	87.91	0.698	
	4	58.16	25.43	1.73	0.47	0.58	0.50	3.58	0.12	90.57	0.718	
	A 1	66.39	22.69	2.35	0.99	0.64	0.04	0.36	0.01	93.46	0.765	
	2	65.72	23.12	2.19	0.82	0.56	0.03	0.36	0.02	92.82	0.760	
	3	66.42	23.32	2.34	1.13	0.54	0.02	0.30	0.02	94.09	0.760	
5-4, 76-79	B 1	71.89	20.91	2.19	1.13	0.54	0.01	0.14	0.01	96.82	0.793	
	2	66.06	22.84	2.30	0.90	0.52	0.02	0.36	0.02	93.01	0.763	
	3	67.06	22.23	2.10	0.58	0.58	0.06	0.54	0.03	93.16	0.770	
	4	65.94	22.86	2.24	0.93	0.58	0.02	0.26	0.02	92.84	0.762	
	C 1	72.22	21.32	2.05	1.10	0.52	0.02	0.12	0.02	97.38	0.790	
	2	66.37	23.35	2.22	1.02	0.56	0.02	0.28	0.02	93.85	0.760	
5-5, 129-132	3	65.63	23.27	2.12	0.81	0.58	0.05	0.50	0.03	92.99	0.758	
	4	70.83	21.92	2.26	1.12	0.53	0.02	0.16	0.01	96.85	0.782	
	5	66.05	23.40	2.30	0.78	0.49	0.02	0.23	0.02	93.30	0.758	
	6	64.00	22.58	2.22	0.87	0.55	0.04	0.38	0.02	90.67	0.759	
	D 1	65.83	22.86	2.08	0.51	0.41	0.02	0.26	0.02	92.00	0.761	
	2	65.71	23.30	2.15	0.60	0.42	0.03	0.29	0.02	92.52	0.758	
5-6, 129-132	3	65.21	23.49	2.18	0.75	0.46	0.02	0.24	0.02	92.37	0.755	
	4	65.76	23.16	2.20	0.77	0.46	0.03	0.37	0.02	92.76	0.760	
	5	65.45	23.18	2.19	0.60	0.45	0.05	0.68	0.04	92.64	0.760	
	6	66.44	22.48	2.07	0.43	0.46	0.04	0.22	0.03	92.16	0.766	
	7	66.16	22.59	2.08	0.44	0.46	0.03	0.25	0.02	92.04	0.764	
	8	65.88	22.79	2.10	0.53	0.53	0.02	0.23	0.03	92.10	0.762	
5-7, 129-132	9	66.21	22.84	2.15	0.51	0.48	0.02	0.23	0.02	92.46	0.763	
	10	66.04	22.91	2.15	0.58	0.50	0.02	0.27	0.02	92.49	0.762	
	11	65.14	22.96	2.17	0.79	0.51	0.03	0.24	0.02	91.86		

Table 1 (continued).

Core-Section interval (cm)	Analysis no. <sup>a</sup>	FeO	TiO <sub>2</sub>	Al <sub>2</sub> O <sub>3</sub>	MgO	MnO	CaO	SiO <sub>2</sub>	K <sub>2</sub> O	Sum	Fe/(Fe + Ti)	Note <sup>b</sup>
6-1, 109-112	B 2	55.44	25.04	1.64	0.55	0.51	0.77	4.82	0.09	88.85	0.711	
	3	52.44	26.37	1.59	0.64	0.47	1.10	7.08	0.14	89.81	0.698	
6-5, 58-61	A 1	67.81	22.12	2.08	0.47	0.60	0.06	0.84	0.07	94.04	0.773	
	2	69.39	21.85	2.19	0.46	0.65	0.06	0.17	0.02	94.80	0.779	
	3	68.01	22.02	2.14	0.46	0.59	0.04	0.49	0.04	93.78	0.774	
	B 1	70.70	21.24	2.30	0.74	0.52	0.07	0.19	0.02	95.78	0.787	
	2	67.76	21.91	2.10	0.39	0.58	0.06	0.23	0.03	93.05	0.775	
	3	67.04	22.04	2.20	0.39	0.59	0.07	0.39	0.03	92.75	0.772	
7-1, 115-118	A 1	73.41	20.43	1.98	0.42	0.54	0.04	0.20	0.02	97.05	0.800	
	2	73.75	20.24	1.91	0.23	0.56	0.06	0.25	0.02	97.03	0.802	
	3	73.71	20.75	1.88	0.32	0.53	0.03	0.22	0.02	97.45	0.798	
	4	73.83	20.42	2.04	0.26	0.49	0.02	0.18	0.02	97.26	0.801	
	B 1	74.05	20.35	2.00	0.17	0.57	0.05	0.21	0.04	97.44	0.802	
	2	73.09	21.36	1.82	0.34	0.52	0.03	0.23	0.03	97.41	0.792	
	3	73.80	20.52	1.79	0.25	0.60	0.05	0.25	0.03	97.29	0.800	
	4	73.39	21.40	1.67	0.25	0.53	0.10	0.22	0.02	97.59	0.792	
7-2, 16-18	A 1	70.67	21.04	1.27	0.27	0.41	0.04	0.37	0.00	94.67	0.789	
	2	71.13	21.86	1.89	0.34	0.41	0.03	0.13	0.00	95.79	0.784	
	3	71.78	21.56	1.76	0.26	0.43	0.01	0.14	0.01	95.94	0.787	
	4	71.49	21.52	1.99	0.23	0.36	0.04	0.18	0.00	95.83	0.787	
	5	71.62	21.21	1.93	0.23	0.40	0.05	0.16	0.00	95.56	0.790	
	B 1	72.40	20.98	1.94	0.33	0.42	0.04	0.13	0.00	96.25	0.793	
	2	72.69	20.15	1.75	0.28	0.45	0.06	0.19	0.00	95.58	0.801	
	3	72.92	20.46	1.80	0.23	0.38	0.16	0.23	0.00	96.18	0.799	
	4	73.65	19.89	1.81	0.22	0.38	0.02	0.17	0.00	96.14	0.845	
	5	72.00	20.94	1.83	0.45	0.37	0.09	0.19	0.00	95.87	0.793	
7-4, 18-21	A 1	71.00	22.12	1.75	0.40	0.56	0.07	0.28	0.02	96.20	0.781	
	2	71.61	21.41	1.69	0.34	0.57	0.09	0.31	0.02	96.05	0.788	
	B 1	73.54	20.16	1.91	0.37	0.53	0.03	0.27	0.01	96.83	0.802	
	2	71.98	20.56	1.90	0.40	0.54	0.09	0.34	0.02	95.83	0.796	
8-3, 130-133	A 1	54.03	42.92	0.45	0.34	0.50	0.01	0.18	0.01	98.44	0.583	
	2	61.86	34.36	0.76	0.23	0.49	0.00	0.21	0.01	97.93	0.667	On lam.
	3	79.57	13.64	1.75	0.15	0.34	0.01	0.18	0.01	95.66	0.866	Betw. lam.
	4	57.48	0.05	0.09	0.00	0.01	0.32	0.01	0.00	58.05	0.999	FeS
	B 1	49.06	49.98	0.08	0.41	0.64	0.00	0.15	0.01	100.34	0.522	On lam.
	2	78.62	13.79	2.08	0.17	0.38	0.02	0.16	0.02	95.23	0.864	Betw. lam.
8-4, 102-105	A 1	74.92	16.90	2.24	0.29	0.48	0.05	0.24	0.02	95.14	0.831	Betw. lam.
	2	79.55	15.50	1.38	0.14	0.30	0.01	0.12	0.02	97.07	0.851	Betw. lam.
	B 1	59.85	0.00	0.04	0.06	0.01	0.28	0.02	0.00	60.26	1.000	FeS
	C 1	80.05	15.12	1.32	0.15	0.37	0.01	0.15	0.03	97.20	0.855	Betw. lam.
	2	61.08	31.83	0.76	0.41	0.71	0.07	1.38	0.04	96.28	0.681	On lam.
	3	56.38	40.62	0.31	0.40	0.63	0.03	0.14	0.02	98.53	0.687	On lam.
8-7, 9-12	A 1	79.09	14.92	1.96	0.23	0.41	0.02	0.13	0.02	96.78	0.855	Betw. lam.
	2	50.79	49.81	0.16	0.60	0.61	0.01	0.14	0.02	102.14	0.531	On lam.
	3	77.78	16.75	1.84	0.27	0.45	0.01	0.13	0.03	97.25	0.838	Betw. lam.
	B 1	59.81	0.00	0.05	0.01	0.01	0.09	0.02	0.00	59.99	1.000	FeS
	C 1	78.30	15.25	1.98	0.20	0.41	0.02	0.17	0.02	96.35	0.851	Betw. lam.
	2	48.53	50.20	0.04	0.77	0.68	0.01	0.12	0.02	100.37	0.518	On lam.
	3	76.53	15.96	2.28	0.30	0.42	0.01	0.20	0.00	95.72	0.842	Betw. lam.
	4	48.83	49.45	0.10	0.95	0.66	0.00	0.15	0.01	100.16	0.523	On lam.
9-3, 88-91	A 1	81.11	11.44	0.64	0.23	0.50	0.04	0.16	0.03	94.14	0.887	
	2	49.50	49.04	0.13	0.81	1.46	0.01	0.18	0.02	101.14	0.529	On lam.
	3	79.50	11.54	1.91	0.33	0.36	0.01	0.16	0.03	93.84	0.885	Betw. lam.
	4	75.50	17.95	1.37	0.42	0.45	0.01	0.19	0.03	95.93	0.824	
	B 1	58.59	35.29	1.01	0.75	1.97	0.02	0.22	0.02	97.87	0.649	On lam.
	2	57.68	35.52	1.05	0.86	1.72	0.03	0.18	0.02	97.06	0.644	On lam.
	3	79.52	12.10	2.23	0.32	0.42	0.02	0.14	0.02	94.76	0.880	On lam.
	4	78.66	12.21	1.65	0.34	0.35	0.04	0.16	0.02	93.43	0.878	Betw. lam.
9-4, 103-106	A 1	80.83	12.83	2.25	0.36	0.35	0.02	0.14	0.02	96.80	0.875	Betw. lam.
	2	57.24	41.42	0.66	0.92	0.60	0.01	0.16	0.02	101.04	0.606	On lam.
	3	60.99	36.99	1.02	0.73	0.57	0.02	0.17	0.02	100.52	0.647	Betw. lam.
	4	81.11	12.21	2.38	0.50	0.35	0.04	0.40	0.02	97.01	0.881	Betw. lam.
	B 1	78.68	14.02	1.51	0.29	0.40	0.04	0.13	0.02	95.09	0.862	Betw. lam.
	2	80.76	13.64	1.12	0.28	0.38	0.02	0.12	0.01	96.33	0.868	Betw. lam.
	3	49.92	49.58	0.12	0.81	0.71	0.01	0.16	0.02	101.33	0.528	On lam.
10-1, 112-115	A 1	75.69	17.47	1.23	0.28	0.44	0.00	0.04	0.02	95.16	0.828	Betw. lam.
	2	47.94	49.18	0.02	0.55	0.64	0.00	0.03	0.02	98.37	0.520	On lam.
	3	75.16	16.81	1.00	0.30	0.47	0.06	0.09	0.03	93.92	0.833	Betw. lam.
	4	47.65	49.29	0.02	0.64	0.65	0.04	0.00	0.01	98.30	0.518	On lam.
	B 1	77.35	16.00	0.89	0.28	0.44	0.02	0.15	0.01	95.13	0.843	Betw. lam.
	2	72.95	17.21	0.77	0.27	0.44	0.04	0.08	0.01	94.78	0.831	
	3	48.22	49.77	0.03	0.64	0.62	0.03	0.12	0.01	99.45	0.519	On lam.
	4	48.14	50.29	0.06	0.82	0.65	0.00	0.00	0.02	99.97	0.516	On lam.
10-5, 84-87	A 1	73.78	20.32	1.10	0.45	0.46	0.01	0.14	0.02	96.28	0.802	
	2	73.06	20.42	1.18	0.50	0.41	0.03	0.14	0.01	95.75	0.799	
	3	74.41	20.28	0.92	0.42	0.46	0.02	0.13	0.01	96.65	0.803	
	B 1	72.95	20.94	1.43	0.67	0.52	0.02	0.12	0.02	96.66	0.795	
	2	72.66	20.79	1.49	0.65	0.58	0.01	0.14	0.02	96.33	0.795	
	3	73.08	21.06	1.24	0.68	0.56	0.02	0.11	0.01	96.76	0.794	
	C	71.99	20.76	1.22	0.66	0.71	0.00	0.03	—	95.37	0.794	
	D	76.51	0.05	0.17	0.03	0.07	0.01	0.09	—	77.93	0.999	FeS
10-7, 42-45	A 1	71.77	20.94	1.29	0.45	0.71	0.04	0.11	0.02	95.32	0.792	
	2	71.69	22.12	1.25	0.66	0.47	0.00	0.07	0.02	96.28	0.783	
	3	71.08	22.28	1.29	0.76	0.58	0.00	0.10	0.02	96.10	0.780	
	4	71.05	22.52	1.34	0.71	0.47	0.00	0.09	0.02	96.20	0.778	
	B 1	72.03	21.86	1.44	0.83	0.49	0.00	0.05	0.01	96.72	0.786	
	2	71.71	21.80	1.50	0.88	0.44	0.00	0.09	0.02	96.45	0.785	
	3	72.71	21.34	1.44	0.75	0.51	0.00	0.10	0.02	96.87	0.791	
11-4, 62-64	A 1	70.59	21.54	2.33	1.81	0.43	0.01	0.12	0.02	96.85	0.785	
	2	74.05	20.56	2.44	1.30	0.44	0.03	0.13	0.01	98.96	0.800	
	3	70.42	22.37	2.22	1.63	0.44	0.02	0.12	0.01	97.23	0.778	
	4	72.28	20.53	2.29	1.73	0.36	0.01	0.11	0.02	97.33	0.797	
	B 1	76.90	15.90	2.62	1.15	0.35	0.02	0.10	0.02	97.08	0.843	Betw. lam.
	2	71.55	21.49	2.21	1.81	0.42						

Table 2. Mean value of each component, Hole 597C samples.

Core-Section, interval (cm) <sup>a</sup>	FeO	TiO <sub>2</sub>	Al <sub>2</sub> O <sub>3</sub>	MgO	MnO	CaO	SiO <sub>2</sub>	K <sub>2</sub> O	Sum
3-1, 131–134	72.83 (1.88)	18.20 (1.19)	2.41 (0.17)	1.01 (0.17)	0.54 (0.14)	0.05 (0.02)	0.31 (0.12)	0.02 (0.00)	95.37 (2.11)
3-2, 40–43	73.92 (0.25)	20.70 (0.27)	2.04 (0.16)	0.33 (0.03)	0.52 (0.02)	0.03 (0.02)	0.26 (0.26)	0.02 (0.01)	97.82 (0.33)
3-3, 5–8	59.17 (5.14)	25.20 (2.79)	1.97 (0.23)	0.60 (0.14)	0.50 (0.09)	0.61 (0.44)	3.44 (1.22)	0.07 (0.01)	91.56 (1.71)
3-3, 52–55	66.38 (0.88)	22.31 (0.48)	2.45 (0.42)	0.27 (0.01)	0.53 (0.05)	0.09 (0.04)	0.38 (0.24)	0.04 (0.01)	92.45 (0.89)
4-1, 60–63	67.26 (2.38)	21.47 (0.90)	2.67 (0.27)	0.89 (0.09)	0.51 (0.06)	0.05 (0.04)	0.99 (2.48)	0.11 (0.24)	93.94 (1.10)
4-2, 111–114	71.71 (1.52)	21.17 (1.48)	2.07 (0.21)	0.36 (0.13)	0.56 (0.04)	0.12 (0.13)	0.17 (0.29)	0.02 (0.01)	96.12 (1.10)
4-3, 27–30	73.71 (0.98)	19.61 (0.52)	2.22 (0.23)	0.44 (0.22)	0.51 (0.05)	0.03 (0.02)	0.05 (0.03)	0.02 (0.01)	96.59 (1.01)
4-4, 76–79	70.25 (1.48)	21.03 (2.34)	2.60 (0.71)	0.48 (0.13)	0.59 (0.09)	0.05 (0.02)	0.15 (0.04)	0.03 (0.01)	95.16 (0.67)
5-1, 129–132	56.81 (2.89)	26.32 (0.73)	1.67 (0.11)	0.55 (0.04)	0.51 (0.07)	0.57 (0.17)	3.17 (0.55)	0.08 (0.02)	89.70 (1.97)
5-2, 63–66	66.35 (1.95)	22.79 (0.59)	2.17 (0.08)	0.79 (0.22)	0.50 (0.06)	0.03 (0.02)	0.34 (0.23)	0.02 (0.01)	93.00 (1.56)
6-1, 109–112	50.25 (3.43)	26.59 (1.25)	1.56 (0.08)	0.63 (0.10)	0.43 (0.08)	1.27 (0.30)	6.90 (1.62)	0.12 (0.03)	87.74 (1.45)
6-5, 58–61	68.45 (1.34)	21.86 (0.32)	2.17 (0.08)	0.49 (0.13)	0.59 (0.04)	0.06 (0.01)	0.39 (0.26)	0.04 (0.02)	94.03 (1.12)
7-1, 115–118	73.63 (0.31)	20.68 (0.45)	1.89 (0.12)	0.28 (0.08)	0.54 (0.03)	0.05 (0.02)	0.22 (0.02)	0.03 (0.01)	97.32 (0.20)
7-2, 16–18	72.04 (0.89)	20.96 (0.63)	1.80 (0.20)	0.28 (0.07)	0.40 (0.03)	0.05 (0.04)	0.19 (0.07)	0.00 (0.00)	95.78 (0.46)
7-4, 18–21	72.03 (1.08)	21.06 (0.88)	1.81 (0.11)	0.38 (0.03)	0.55 (0.02)	0.07 (0.03)	0.30 (0.03)	0.02 (0.01)	96.23 (0.43)
8-3, 130–133(o)	55.46 (9.05)	42.17 (11.05)	0.42 (0.48)	0.32 (0.13)	0.57 (0.11)	0.00 (0.00)	0.18 (0.04)	0.01 (0.00)	99.14 (1.70)
(b)	79.10 (0.67)	13.72 (0.11)	1.92 (0.23)	0.16 (0.01)	0.36 (0.03)	0.02 (0.01)	0.17 (0.01)	0.02 (0.01)	95.45 (0.30)
8-4, 102–105(o)	58.73 (3.32)	36.23 (6.22)	0.54 (0.32)	0.41 (0.01)	0.67 (0.06)	0.05 (0.03)	0.76 (0.88)	0.03 (0.01)	97.41 (1.59)
(b)	78.17 (2.83)	15.84 (0.94)	1.65 (0.51)	0.19 (0.08)	0.38 (0.09)	0.02 (0.03)	0.17 (0.06)	0.02 (0.01)	96.45 (1.14)
8-7, 9–12(o)	49.38 (1.23)	49.82 (0.38)	0.07 (0.04)	0.77 (0.18)	0.65 (0.04)	0.01 (0.01)	0.14 (0.02)	0.02 (0.01)	100.89 (1.09)
(b)	77.93 (1.07)	15.72 (0.81)	0.22 (0.16)	0.25 (0.04)	0.42 (0.02)	0.02 (0.01)	0.16 (0.03)	0.02 (0.01)	96.53 (0.65)
9-3, 88–91(o)	55.26 (5.01)	39.95 (7.87)	0.73 (0.52)	0.81 (0.06)	1.72 (0.26)	0.02 (0.01)	0.19 (0.02)	0.02 (0.00)	98.69 (2.16)
(b)	78.86 (2.08)	13.05 (2.76)	1.56 (0.60)	0.33 (0.07)	0.42 (0.06)	0.02 (0.02)	0.16 (0.02)	0.03 (0.01)	94.42 (0.97)
9-4, 103–106(o)	56.05 (5.63)	42.66 (6.39)	0.60 (0.45)	0.82 (0.10)	0.63 (0.07)	0.01 (0.01)	0.16 (0.01)	0.02 (0.00)	100.96 (0.41)
(b)	80.35 (1.12)	13.18 (0.81)	1.82 (0.60)	0.36 (0.10)	0.37 (0.02)	0.03 (0.01)	0.20 (0.14)	0.02 (0.01)	96.31 (0.86)
10-1, 112–115(o)	47.99 (0.25)	49.63 (0.51)	0.03 (0.02)	0.66 (0.11)	0.64 (0.01)	0.02 (0.02)	0.04 (0.06)	0.02 (0.01)	99.02 (0.82)
(b)	76.04 (0.93)	16.87 (0.64)	0.97 (0.20)	0.28 (0.01)	0.45 (0.02)	0.03 (0.03)	0.09 (0.05)	0.02 (0.01)	94.75 (0.58)
10-5, 84–87	73.13 (0.78)	20.65 (0.31)	1.23 (0.19)	0.58 (0.11)	0.53 (0.10)	0.02 (0.01)	0.12 (0.04)	0.02 (0.01)	96.26 (0.52)
10-7, 42–45	71.72 (0.57)	21.84 (0.55)	1.36 (0.10)	0.72 (0.14)	0.52 (0.09)	0.01 (0.02)	0.09 (0.02)	0.02 (0.00)	96.28 (0.51)
11-4, 62–64	71.75 (1.32)	21.34 (0.70)	2.32 (0.10)	1.75 (0.29)	0.42 (0.03)	0.01 (0.01)	0.12 (0.01)	0.02 (0.01)	97.71 (0.78)
(b)	76.90 (0.00)	15.90 (0.00)	2.62 (0.00)	1.15 (0.00)	0.35 (0.00)	0.02 (0.00)	0.10 (0.00)	0.02 (0.00)	97.08 (0.00)

Note: All data are expressed in wt.%. Parentheses indicate standard deviations.

<sup>a</sup> (a) means that the position of an analysis point is on a lamella. (b) means that the position of an analysis point is between lamellae.

dicate standard deviations. Lamellae were observed in Sample 597C-8-3, 130–133 cm and in samples from deeper in the hole; mean values for such samples are given in Table 2 for measurements (o) on lamellae and (b) between lamellae. Figure 1 shows the variation of each component as a function of depth; bars indicate standard deviations. The weight percentages of MnO, CaO, SiO<sub>2</sub>, and K<sub>2</sub>O are almost constant. Generally, the values of Al<sub>2</sub>O<sub>3</sub> and MgO decrease with depth in the hole. The ratio of Fe to Ti was calculated and is shown in Table 3 as Fe/(Fe + Ti).

Titanomagnetites are often found to be the carriers of remanent magnetization in most natural rocks. The composition parameter *x* is used to indicate the proportion of ulvöspinel in the titanomagnetite solid solution series, and is defined by

$$x\text{Fe}_2\text{TiO}_4 \cdot (1 - x)\text{Fe}_3\text{O}_4 \quad (0 \leq x \leq 1).$$

*x* = 0.0 indicates magnetite and *x* = 1.0 indicates ulvöspinel. Submarine basalts are often reported to contain about 60% ulvöspinel, whereas continental basalts are reported to contain nearly none (Marshall, 1978; Kono, 1980).

The *x* values can be obtained in the FeO–Fe<sub>2</sub>O<sub>3</sub>–TiO<sub>2</sub> system, ignoring other components. Fe/(Fe + Ti) and *x* are represented as a function of depth in Figure 2. This figure shows that the titanomagnetite composition (*x*) for samples from Hole 597C is generally 0.6 to 0.7; the

mean value of *x* is 0.68 ± 0.12. This value is similar to that reported for previous DSDP samples.

#### THERMOMAGNETIC ANALYSIS AND ESTIMATION OF THE OXIDATION PARAMETER

Thermomagnetic curves were obtained for 24 samples in a magnetic field of 4 kOe. A 200- to 400-mg sample was heated in the balance, which was constantly evacuated (below 1 × 10<sup>-5</sup> Torr), at temperatures up to 650°C. Some thermomagnetic curves are shown in Figures 3, 4, and 5.

It is inferred that, as indicated by the existence of lamellae, samples from deeper than 100 m had been affected by high-temperature oxidation. For example, the thermomagnetic curves for Samples 597C-9-3, 88–91 cm (113.39 m) and 597C-9-4, 103–106 cm (115.05 m) (Fig. 3) show high Curie temperatures in the heating process, and the heating and cooling curves are almost the same, indicating the effect of high-temperature oxidation. All samples from below 100 m show similar evidence of high-temperature oxidation.

Heating curves for Samples 597C-3-1, 131–134 cm (56.83 m) and 597C-4-1, 60–63 cm (65.12 m) (Fig. 4) are cone-shaped at temperatures above 400°C, and the cooling curves, whose Curie temperatures are above 500°C, steepen sharply. These curves are typical of samples affected by low-temperature oxidation. Judging from the thermomagnetic curves, other examples of low-temperature oxidation products are Hole 597C Samples 3-1, 131–

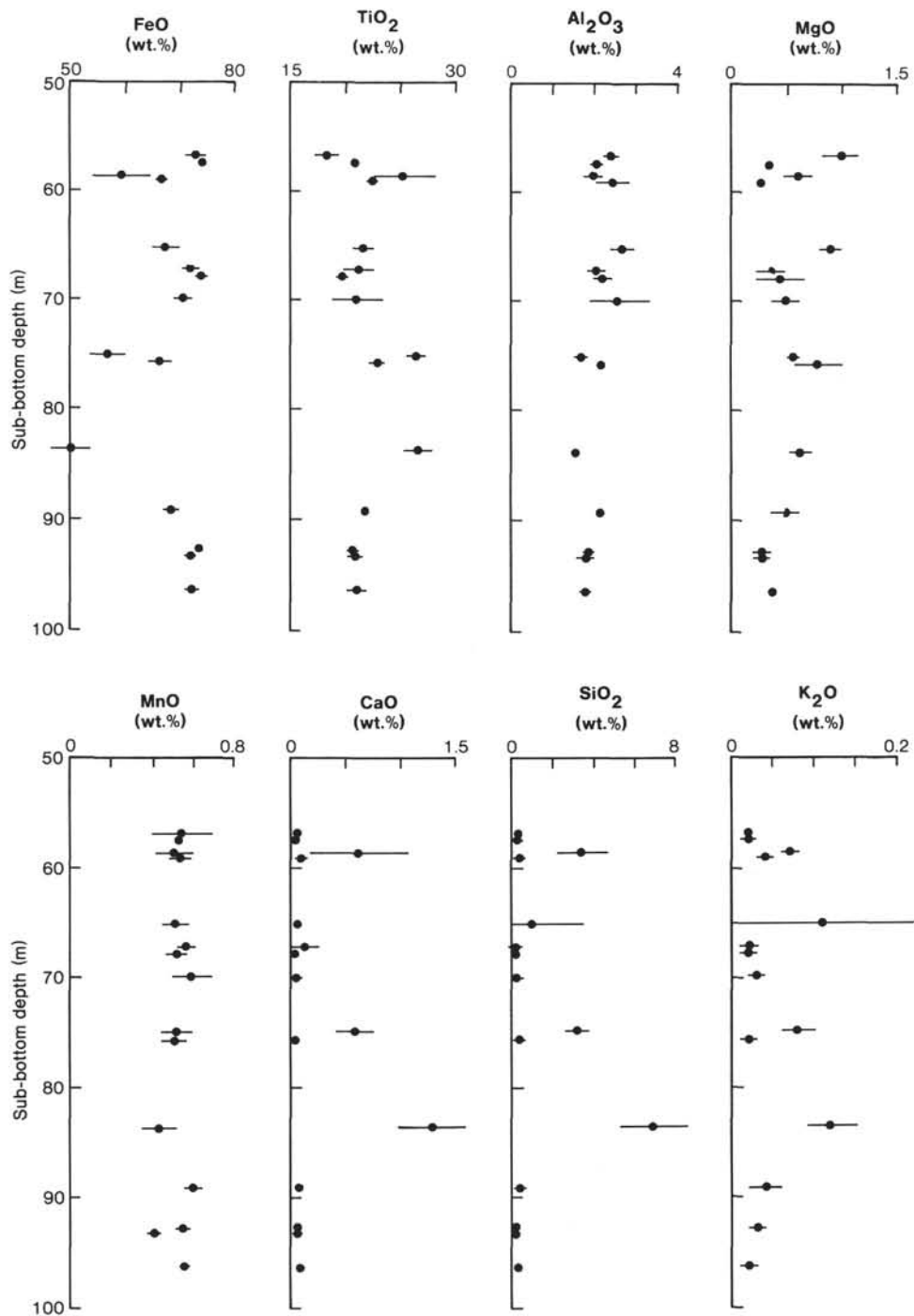


Figure 1. Variation of components FeO, TiO<sub>2</sub>, Al<sub>2</sub>O<sub>3</sub>, MgO, MnO, CaO, SiO<sub>2</sub>, and K<sub>2</sub>O as a function of depth. Bars indicate standard deviations.

134 cm; 3-3, 5-8 cm; 3-3, 52-55 cm; 4-1, 60-63 cm; 4-4, 76-79 cm; 5-1, 129-132 cm; 5-2, 63-66 cm; 6-1, 109-112 cm; 6-5, 58-61 cm; and 7-4, 18-21 cm.

In contrast, Samples 597C-4-3, 27-30 cm (67.79 m) and 597C-7-1, 115-118 cm (92.67 m) showed little effect from low-temperature oxidation; the thermomagnetic curves are almost interchangeable, indicating low Curie temperatures of 160 to 210°C (Fig. 5).

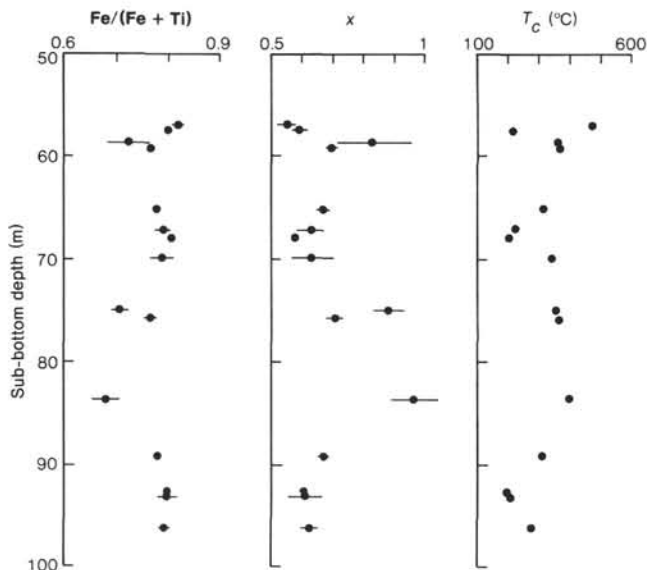
For low-temperature oxidation, oxidation parameter  $\gamma$  can be estimated from the  $T_c$ - $z$  diagram of Nishitani

and Kono (1983), using the  $x$  values obtained by microprobe analyses and the Curie temperatures obtained from thermomagnetic curves. Nishitani (1981) showed, however, that the Curie temperature decreases as the amount of Al and/or Mg increases. Electron microprobe analyses show that the amount of Al<sub>2</sub>O<sub>3</sub> in Hole 597C basalts is much greater than the amount of MgO, so the effect of MgO is ignored here. The concentration of Al<sub>2</sub>O<sub>3</sub> is about 2 wt.%, which may decrease the Curie temperature by a maximum of 50°C. Thus, the Curie tempera-

Table 3. The ratio  $\text{Fe}/(\text{Ti} + \text{Ti})$ ,  $x$ , Curie temperature, and oxidation parameter  $z$ , Hole 597C samples.

Core-Section, interval (cm)	$\text{Fe}/(\text{Fe} + \text{Ti})$	$x$	$T_1$	$T_2$	$T_3$	$z_1$	$z_2$	Sub-bottom depth (m)
3-1, 131-134	0.817 (0.010)	0.550 (0.030)	468	578	545	0.90	0.33 (0.42)	56.83
3-2, 40-43	0.799 (0.002)	0.594 (0.025)	219	152	0.18	-0.04 (0.17)		57.42
3-3, 5-8	0.722 (0.040)	0.834 (0.119)	356	577	541	-	1.31 (0.36)	58.57
3-3, 52-55	0.768 (0.006)	0.697 (0.017)	364	589	538	0.77	1.03 (0.18)	59.04
4-1, 60-63	0.777 (0.007)	0.669 (0.021)	315	506	518	0.60	0.74 (0.23)	65.12
4-2, 111-114	0.790 (0.014)	0.629 (0.043)	226		350	0.30	0.25 (0.19)	67.13
4-3, 27-30	0.807 (0.005)	0.579 (0.016)	201		160	0.10	0.10 (0.21)	67.79
4-4, 76-79	0.788 (0.022)	0.635 (0.067)	340	518	492	0.62	0.45 (0.12)	69.78
5-1, 129-132	0.706 (0.016)	0.883 (0.049)	355	577	545	-	1.71 (0.41)	74.81
5-2, 63-66	0.764 (0.009)	0.708 (0.027)	366	592	546	0.78	0.93 (0.32)	75.64
6-1, 109-112	0.678 (0.026)	0.966 (0.077)	401	586	550	-	2.23 (0.31)	83.61
6-5, 58-61	0.777 (0.006)	0.670 (0.017)	316	563	532	0.61	0.70 (0.23)	89.10
7-1, 115-118	0.798 (0.004)	0.605 (0.012)	200		165	0.13	0.002 (0.03)	92.67
7-2, 16-18	0.797 (0.018)	0.610 (0.053)	210		163	0.18	0.31 (0.10)	93.17
7-4, 18-21	0.792 (0.009)	0.625 (0.028)	275	508	483	0.40	0.23 (0.10)	96.20
8-3, 130-133	-	-	500	408	-	-		104.82
8-4, 102-105	-	-	484	382	-	-		106.04
8-7, 9-12	-	-	449	422	-	-		109.61
9-3, 88-91	-	-	556	519	-	-		113.39
9-4, 103-106	-	-	506	456	-	-		115.05
10-1, 112-115	-	-	504	335	-	-		119.64
10-5, 84-87	-	-	492	502	-	-		125.36
10-7, 42-45	-	-	497	449	-	-		127.93
11-4, 62-64	-	-	508	308	-	-		132.63

Note:  $T_1$  = the first Curie temperatures observed during heating.  $T_2$  = the highest Curie temperatures observed during heating.  $T_3$  = Curie temperatures observed during cooling.  $z_1$  = oxidation parameters determined using the  $T_c-z$  diagram of Nishitani and Kono (1983).  $z_2$  = oxidation parameters determined by electron microprobe analysis, assuming that the difference 100 minus the total percentage by weight is excess oxygen. Parentheses indicate standard deviations. Dashes indicate that values were not obtained; blanks in  $T_2$  indicate that the second peak was not observed in a heating process.

Figure 2.  $\text{Fe}/(\text{Fe} + \text{Ti})$ ,  $x$  values, and Curie temperature ( $T_c$ ), as functions of depth. Bars indicate standard deviations.

tures determined from thermomagnetic curves may be offset by the presence of  $\text{Al}_2\text{O}_3$ , and the estimates of the titanomagnetite oxidation parameter  $z$  may consequently be in error.

There is another way to calculate the oxidation parameter. This is to assume that the difference of 100 minus the total percentage by weight is excess oxygen. Values obtained by this method are shown in Table 3 as  $z_2$ .

This method leads to excessive error, however: Sample 597C-3-2, 40-43 cm indicates a negative oxidation state, and Samples 597C-3-3, 5-8 cm, 597C-3-3, 52-55 cm, 597C-5-1, 129-132 cm, and 597C-6-1, 109-112 cm indicate  $z_2$  values greater than one. It is therefore assumed here that better estimates of the oxidation parameter can be obtained using Curie temperatures and the Fe to Ti ratios, although this method ignores the effects of impurities.

The amounts of the oxidation product so obtained are listed in Table 3 as  $z_1$  and plotted on Figure 6. The  $z$  values for samples affected by low-temperature oxidation vary widely, but they have a tendency to decrease as depth increases.

As already described, samples from deeper than 100 m had been affected by high-temperature oxidation, judging by microscopic observation of lamellae and by the characteristics of the thermomagnetic analysis. We can conclude that the magnetic properties of Hole 597C change at 100 m sub-bottom depth, and that low-temperature and high-temperature oxidation processes prevailed above 100 m and below 100 m, respectively.

## REFERENCES

- Bence, A. E., and Albee, A. L., 1968. Empirical correction factors for the electron microanalysis of silicates and oxides. *J. Geol.*, 76:382-403.
- Buddington, A. F., and Lindsley, D. H., 1964. Iron-titanium oxide minerals and synthetic equivalents. *J. Petrol.*, 5:310-357.
- Hamano, Y., Nishitani, T., and Kono, M., 1980. Magnetic properties of basalt samples from Deep Sea Drilling Project Holes 417D and 418A. In Donnelly, T., Francheteau, J., Bryan, W., Robinson, P.,

- Flower, M., Salisbury, M., et al., *Init. Repts. DSDP*, 51, 52, 53, Pt. 2: Washington (U.S. Govt. Printing Office), 1391-1405.
- Hauptman, Z., 1974. High temperature oxidation, range of non-stoichiometry and Curie point variation of cation deficient titanomagnetite  $\text{Fe}_{2.4}\text{Ti}_{0.6}\text{O}_4 + \gamma$ . *Geophys. J. R. Astron. Soc.*, 38:29-47.
- Kono, M., 1980. Magnetic properties of DSDP Leg 55 basalts. In Jackson, E. D., Koizumi, I., et al., *Init. Repts. DSDP*, 55: Washington (U.S. Govt. Printing Office), 723-736.
- Marshall, M., 1978. The magnetic properties of some DSDP basalts from the North Pacific and inferences for Pacific Plate tectonics. *J. Geophys. Res.*, 83:289-308.
- Nishitani, T., 1981. Magnetic properties of titanomagnetites containing spinel ( $\text{MgAl}_2\text{O}_4$ ). *J. Geomagn. Geoelectr.*, 33:171-179.
- Nishitani, T., and Kono, M., 1983. Curie temperature and lattice constant of oxidized titanomagnetite. *Geophys. J. R. Astron. Soc.*, 74:585-600.
- Ozima, M., and Ozima, M., 1971. Characteristic thermomagnetic curve in submarine basalts. *J. Geophys. Res.*, 76:2051-2056.
- Ozima, M., and Sakamoto, N., 1971. Magnetic properties of synthesized titanomaghemitite. *J. Geophys. Res.*, 76:7035-7046.

Date of Initial Receipt: 16 July 1984

Date of Acceptance: 26 December 1984

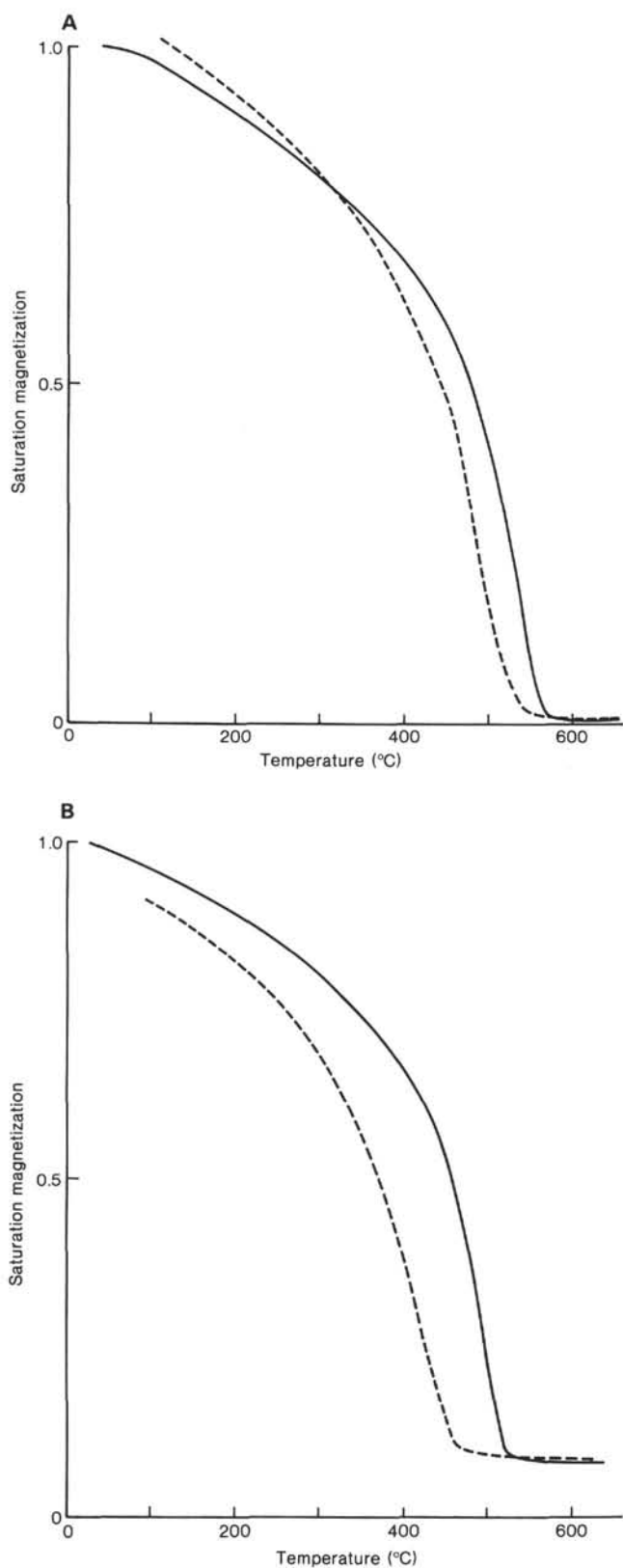


Figure 3. Thermomagnetic curves. Solid lines indicate heating process and dotted lines indicate cooling process. A. Sample 597C-9-3, 88–91 cm (113.39 m). B. Sample 597C-9-4, 103–106 cm (115.05 m).

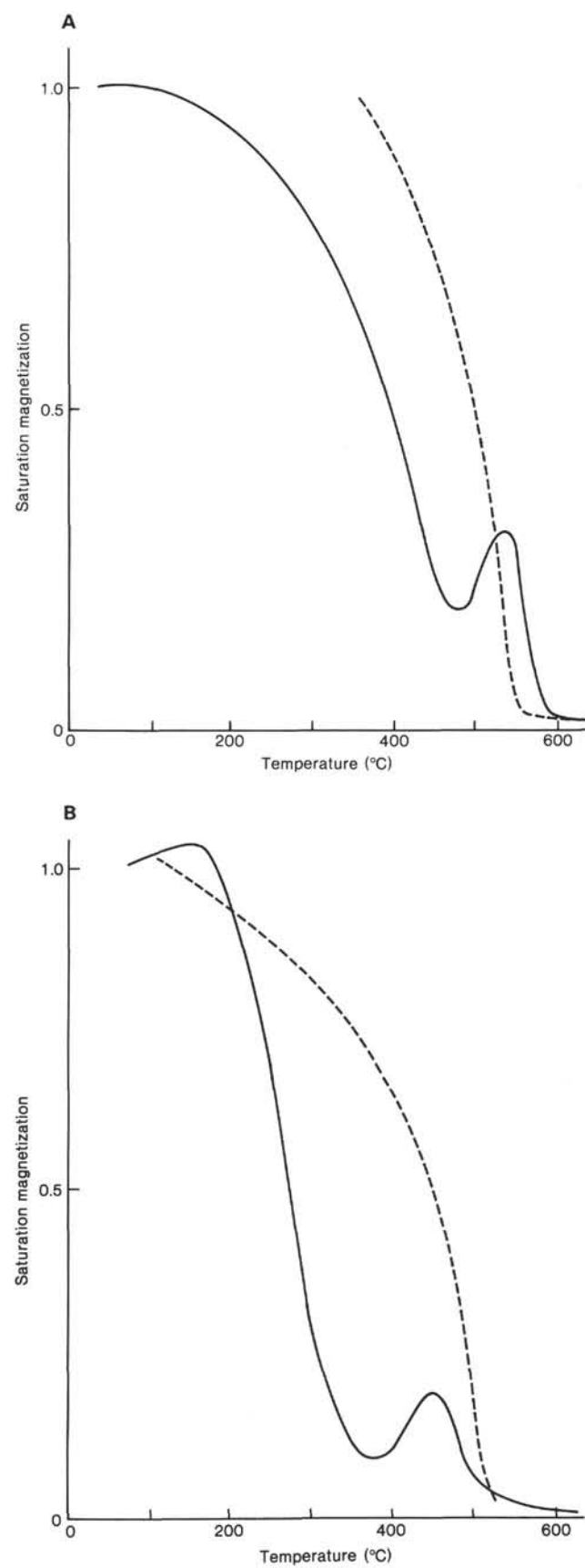


Figure 4. Thermomagnetic curves. Solid lines indicate heating process and dotted lines indicate cooling process. A. Sample 597C-3-1, 131–134 cm (56.83 m). B. Sample 597C-4-1, 60–63 cm (65.12 m).

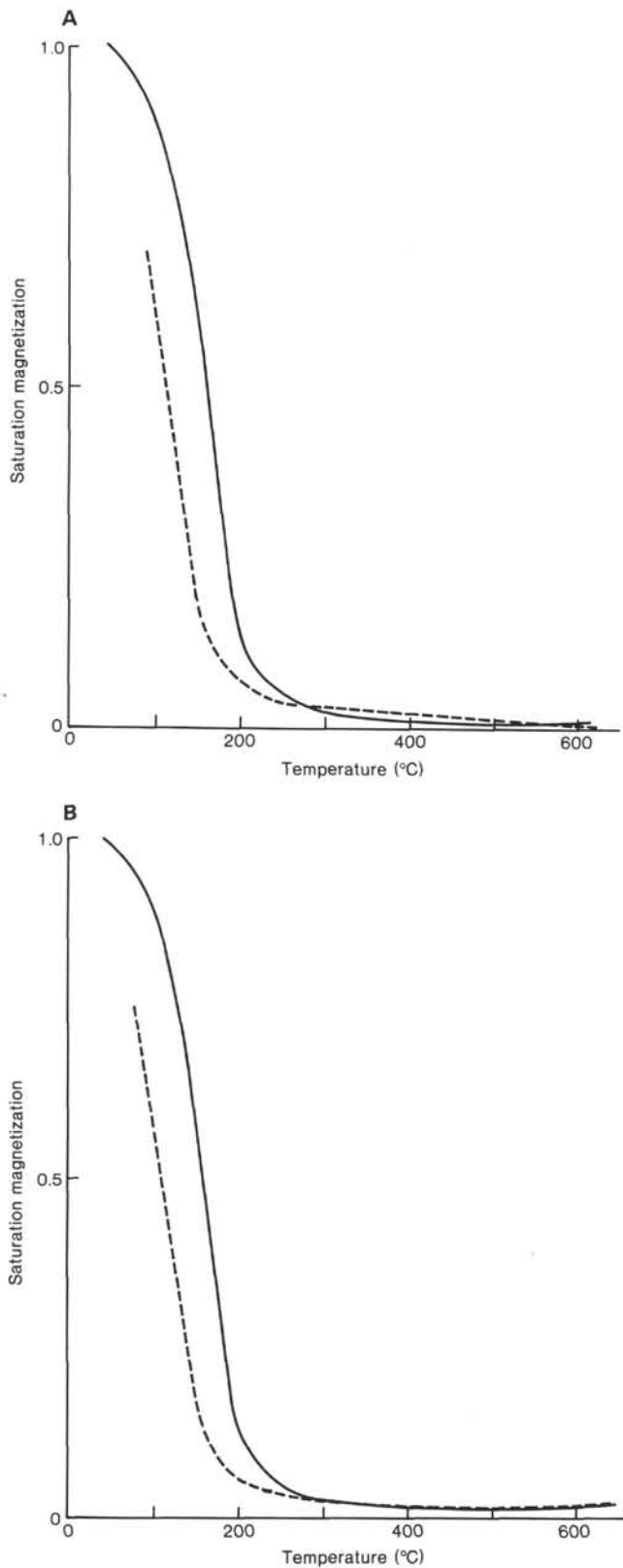


Figure 5. Thermomagnetic curves. Solid lines indicate heating process and dotted lines indicate cooling process. A. Sample 597C-4-3, 27-30 cm (67.79 m). B. Sample 597C-7-1, 115-118 cm (92.67 m).

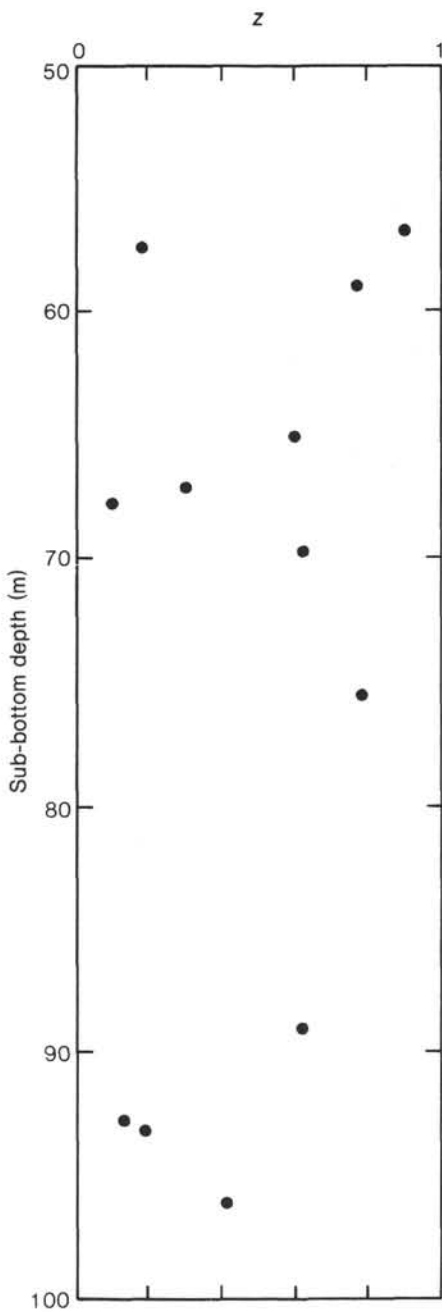


Figure 6. Oxidation parameter ( $z$ ) as a function of depth.